Free Rad. Res., Vol. 23, No. 2, pp. 151–172
Reprints available directly from the publisher
Photocopying permitted by license only

KINETIC MODELLING OF *IN VITRO* LIPID PEROXIDATION EXPERIMENTS – 'LOW LEVEL' VALIDATION OF A MODEL OF *IN VIVO* LIPID PEROXIDATION

ARMINDO SALVADOR[#]*, FERNANDO ANTUNES[#] and RUY E. PINTO[#,@]

[#]*Grupo de Bioquímica e Biologia Teóricas, Instituto de Investigação Científica Bento da Rocha Cabral, Cç. Bento da Rocha Cabral, 14, P-1200 Lisboa, Portugal.*
[@]*Departamento de Química e Bioquímica da Faculdade de Ciências da Universidade de Lisboa, R. Ernesto de Vasconcelos, Edifício C1, 5° piso, P-1700 Lisboa, Portugal*

(Received September 16th, 1994; in revised form, November 9th, 1994)

Kinetic modelling overcomes some of the drawbacks of purely intuitive thinking in integrating information accumulated on chemical reactions involved in oxidative stress. However, it is important to assess if current knowledge about the reactions that mediate lipid peroxidation already allows satisfactory modelling of this process in near-to-physiological conditions. In this paper, a set of increasingly complex *in vitro* experiments on antioxidants (α-tocopherol and ascorbate) and lipid peroxidation in heterogeneous systems is simulated. Quantitative to semiquantitative agreement is found between experimental and simulation results. In addition, this theoretical analysis provided useful insights, suggested new hypotheses and experiments and pointed out relevant aspects needing further research. The results encourage and serve as partial validation for the formulation of relatively detailed mathematical models of *in vivo* lipid peroxidation. Some important aspects of the formulation and analysis of such models are discussed.

KEY WORDS: oxidative stress, antioxidants, α-tocopherol, ascorbate, free radicals, computer simulation.

Abbreviations and symbols: Asc, dehydroascorbate; $Asc^{\bullet-}$, semidehydroascorbate radical; $AscH^-$, ascorbate monoanion; DLPC, L-α-1,2-dilinoleoylphosphatidylcholine; k_n, rate constant for reaction number n; k_p, rate constant for propagation; k_t, rate constant for second order termination; $L^\bullet$, fatty acyl carbon centred radical; LH, unsaturated fatty acyl; LHn, unsaturated fatty acyl with n double bounds; $LO^\bullet$, fatty acyl alkoxyl radical; LOH, hydroxy-fatty acyl; $LOO^\bullet$, fatty acyl peroxyl radical; LOOH, fatty acyl hydroperoxide; n_x, number of moles of substance X; PUFA, polyunsaturated fatty acid; R_i, rate of initiation of lipid peroxidation; $ROO^\bullet$, peroxyl radical of aqueous phase initiator of lipid peroxidation; ROO^-, hydroperoxide anion of aqueous phase initiator; ROOH, hydroperoxide of aqueous phase initiator; R_p, rate of production of lipid hydroperoxides; SOD, superoxide dismutase; TBARS, thiobarbituric acid reactive substances; $TocO^\bullet$, α-tocopheroxyl radical; TocOH, α-tocopherol; V_{aq}, volume of the aqueous phase; V_m, volume of the membrane phase; X_{aq}, species in aqueous phase; X_m, species in membrane phase.

INTRODUCTION

A great amount of quantitative kinetic data on reactions related to lipid peroxidation has been collected over the last decades. However, the complexity of this metabolic process sometimes makes difficult to understand intuitively if and how the observed

*Author for correspondence

experimental responses arise from those known reactions. On the other hand, such data enable the setting up of reasonably detailed kinetic models. These mathematical models are a more rigorous formal setting that overcomes many of the limitations of purely intuitive reasoning. So, they can be more successful in addressing the above mentioned issues. Several workers[1–16†] have already applied this approach to the study of lipid peroxidation and oxygen activation.

In vivo lipid peroxidation occurs in an heterogeneous open system (with permanent exchange of lipids,[17,18] oxidants, antioxidants and peroxidation products between membranes and their environment) and under the influence of a multitude of enzymatic activities. These factors usually interact in complicated ways. Even very elaborate *in vitro* experiments are far from reproducing such conditions. Therefore, the extrapolation of *in vitro* results on to the biological environment is *not* straightforward. In this regard, quantitative determinations of kinetic parameters of individual reactions, though less informative about integrative aspects, seem more robust than results from *in vitro* studies of the responses of more 'complete' systems. However, if well controlled, the latter experiments may be useful in revealing gaps and inconsistencies on the knowledge about the reactional mechanisms of such responses, as explained below.

Mathematical models of oxidative stress in 'intact' biological systems integrate data from chemical kinetics and bridge it to studies of physiological responses. Taking the preceding discussion into account, it can be conjectured that such models may prove themselves very effective in deepening our understanding of biological oxidative stress. Setting them up, however, requires careful selection of the available data. Some assumptions have also to be made, either for the sake of simplicity or to cover eventual gaps of knowledge. Therefore, a systematic evaluation of the quality of the data and of the assumptions is necessary. One way of doing it, is to assess the performance of simpler, suitably adapted, (sub)models in predicting the behaviour of *in vitro* peroxidation systems with intermediate degrees of complexity. We call this approach 'low level validation'.

In this work, increasingly complex published *in vitro* experiments on lipid peroxidation and antioxidants are simulated using a set of kinetic models. The theoretical results show acceptable agreement with the experimental observations, giving support to the use of (more complicated) mathematical models of specific biological environments. In addition, the theoretical analysis of the experiments provided useful insights into the processes under scrutiny and suggested new hypotheses and experiments.

Some important aspects concerning the formulation and analysis of complex models of *in vivo* oxidative stress are discussed.

METHODS

A set of experiments involving different aspects of lipid peroxidation and of the action of several antioxidants was simulated. Whenever possible, experiments done under well-controlled conditions and allowing a direct quantitative comparison between experimental and simulation results were chosen. The independent variables and initial conditions have been estimated so that the particular conditions of each experiment could be reproduced. *No further adjustments or fittings were made.*

†See also: A.L. Tappel, A.A. Tappel and C. Fraga (1989) Application of simulation modeling to lipid peroxidation processes. *Free Radical Biology and Medicine*, **7**, 361–368.

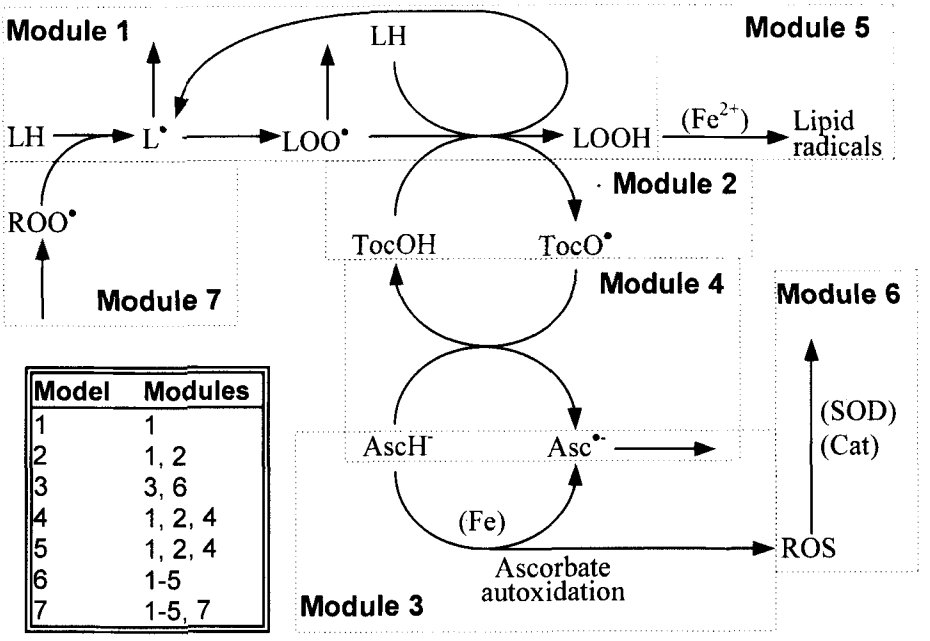

Model	Modules
1	1
2	1, 2
3	3, 6
4	1, 2, 4
5	1, 2, 4
6	1-5
7	1-5, 7

FIGURE 1 Simplified diagram of the processes under consideration by the different models in this work. The table in inset shows which modules are accounted for in each model. The reactions in each module are described in Table 1. Cat and ROS stand for catalase and reactive oxygen species, respectively.

With one exception, only experiments using heterogeneous systems have been chosen. This was done because this work is intended to contribute to a 'low level' validation of a model[19] for lipid peroxidation in biological membranes.

A lipid and an aqueous compartment (with volumes V_m and V_{aq}, respectively) were considered in the simulations, each with a characteristic composition and reactivity. All lipid species and α-tocopherol are only present in the lipid phase. $HO_2^{\bullet}$ and O_2 are considered to distribute instantaneously between the two compartments, with partition coefficients (lipid to aqueous phase) of 1 and 3[ref. 20] respectively. All other species are assumed to be present only in the aqueous phase. Some interfacial reactions are allowed. Unless otherwise stated, local concentrations referred to the compartment where the species is present are considered. The rates of interfacial reactions are referred to the membrane phase. Multiplication of these rates by V_m/V_{aq} and by the appropriate stoichiometric factor yields the rates of change of the concentrations of the aqueous species due to those reactions. The mathematical treatment of compartmentation is described in further detail in[19].

All reactions were assumed to obey mass action kinetics.

A general diagram of the processes considered in each model is presented (Figure 1). The respective sets of reactions and rate constants are shown in Table 1. Further details pertaining to each model are given in the Results section. More extended discussions about the estimation and biological relevance of the rate constants appear in[19].

Setting up of the models, implementation of the systems of ordinary differential equations, simulations and analyses were carried out using PARSYS,[ref. 66] a set of

TABLE 1
Reactions and rate constants considered in the simulations.

Module	No	Reaction	Rate constant	Source
	1	$LH1 \rightarrow L^{\cdot}$	[a]	
	2	$LH2 \rightarrow L^{\cdot}$	[a]	
	3	$LH3 \rightarrow L^{\cdot}$	[a]	
	4	$LH4 \rightarrow L^{\cdot}$	[a]	
	5	$LH5 \rightarrow L^{\cdot}$	[a]	
	6	$LH6 \rightarrow L^{\cdot}$	[a]	
	7	$L^{\cdot} + L^{\cdot} \rightarrow$ Products	$10^6\ M^{-1}s^{-1}$	Estimated from data in[21,22]
	8	$L^{\cdot} + O_2 \rightarrow LOO^{\cdot}$	$2.2 \times 10^8 M^{-1}s^{-1}$	Estimated from data in[23,24]
1	9	$LOO^{\cdot} \rightarrow L^{\cdot} + O_2$	$150s^{-1}$	[25]
	10	$L^{\cdot} + LOO^{\cdot} \rightarrow$ Products	$5 \times 10^5 M^{-1}s^{-1}$	Estimated from data in[21,26]
	11	$LOO^{\cdot} + LOO^{\cdot} \rightarrow$ Products	$10^5\ M^{-1}s^{-1}$	Estimated from data in[21]
	12	$LH1 + LOO^{\cdot} \rightarrow L^{\cdot} + LOOH$	$9 \times 10^{-3} M^{-1}s^{-1}$	Estimated from data in[21,27]
	13	$LH2 + LOO^{\cdot} \rightarrow L^{\cdot} + LOOH$	$18.05\ M^{-1}s^{-1}$	[21]
	14	$LH3 + LOO^{\cdot} \rightarrow L^{\cdot} + LOOH$	$38.08\ M^{-1}s^{-1}$	Estimated from data in[21,27]
	15	$LH4 + LOO^{\cdot} \rightarrow L^{\cdot} + LOOH$	$47.9\ M^{-1}s^{-1}$	Estimated from data in[21,27]
	16	$LH5 + LOO^{\cdot} \rightarrow L^{\cdot} + LOOH$	$68.83\ M^{-1}s^{-1}$	Estimated from data in[21,27]
	17	$LH6 + LOO^{\cdot} \rightarrow L^{\cdot} + LOOH$	$89.75\ M^{-1}s^{-1}$	Estimated from data in[21,27]
	18	$LOO^{\cdot} + TocOH \rightarrow LOOH + TocO^{\cdot}$	$5.8 \times 10^3 M^{-1}s^{-1}$	[28]
	19	$LH1 + TocO^{\cdot} \rightarrow L^{\cdot} + TocOH$	$0.1\ M^{-1}s^{-1}$	Estimated from data in[29]
	20	$LH2 + TocO^{\cdot} \rightarrow L^{\cdot} + TocOH$	$0.1\ M^{-1}s^{-1}$	Estimated from data in[29]
	21	$LH3 + TocO^{\cdot} \rightarrow L^{\cdot} + TocOH$	$0.1\ M^{-1}s^{-1}$	Estimated from data in[29]
2	22	$LH4 + TocO^{\cdot} \rightarrow L^{\cdot} + TocOH$	$0.1\ M^{-1}s^{-1}$	Estimated from data in[29]
	23	$LH5 + TocO^{\cdot} \rightarrow L^{\cdot} + TocOH$	$0.1\ M^{-1}s^{-1}$	Estimated from data in[29]
	24	$LH6 + TocO^{\cdot} \rightarrow L^{\cdot} + TocOH$	$0.1\ M^{-1}s^{-1}$	Estimated from data in[29]
	25	$LOO^{\cdot} + TocO^{\cdot} \rightarrow$ Products	$2.5 \times 10^6 M^{-1}s^{-1}$	[30]
	26	$TocO^{\cdot} + TocO^{\cdot} \rightarrow$ Products	$10^4\ M^{-1}s^{-1}$	[30]
	27	$LOOH + TocO^{\cdot} \rightarrow LOO^{\cdot} + TocOH$	$1\ M^{-1}s^{-1}$	Estimated from data in[27,31]
	28	$Fe^{2+} + O_2 \rightarrow Fe^{3+} + O_2^{\cdot-}$	$6 \times 10^2 M^{-1}s^{-1}$	[32]
	29	$Fe^{3+} + O_2^{\cdot-} \rightarrow Fe^{2+} + O_2$	$2 \times 10^6 M^{-1}s^{-1}$	[32]
	30	$Fe^{2+} + O_2^{\cdot-} + 2\,H^+ \rightarrow Fe^{3+} + H_2O_2$	$2 \times 10^6\ M^{-1}s^{-1}$	[32]
	31	$Fe^{3+} + H_2O_2 \rightarrow Fe^{2+} + O_2^{\cdot-} + 2\,H^+$	$3.5 \times 10^2\ M^{-1}s^{-1}$	[32]
	32	$Fe^{2+} + H_2O_2 \rightarrow Fe^{3+} + HO^{\cdot} + HO^-$	$2 \times 10^4 M^{-1}s^{-1}$	[32]
3	33	$Fe^{2+} + HO^{\cdot} \rightarrow Fe^{3+} + HO^-$	$3.4 \times 10^8\ M^{-1}s^{-1}$	[33]
	34	$H_2O_2 + HO^{\cdot} \rightarrow HO_2^{\cdot}a + H_2O$	$3.4 \times 10^7\ M^{-1}s^{-1}$	Estimated from data in[34,35]
	35	$HO^{\cdot} + O_2^{\cdot-} + H^+ \rightarrow O_2 + H_2O$	$10^{10}\ M^{-1}s^{-1}$	[36]
	36	$AscH^- + Fe^{3+} \rightarrow Fe^{2+} + Asc^{\cdot-} + H^+$	$5 \times 10^2\ M^{-1}s^{-1}$	Estimated from data in [32,37,38]
	37	$AscH^- + HO^{\cdot} \rightarrow H_2O + Asc^{\cdot-}$	$10^{10}\ M^{-1}s^{-1}$	Estimated from data in[39]
	38	$Asc^{\cdot-} + Fe^{3+} \rightarrow Asc + Fe^{2+}$	$4 \times 10^6\ M^{-1}s^{-1}$	[38]
	39	$HO_2^{\cdot}a \rightarrow O_2^{\cdot-} + H^+$	$5.02 \times 10^7 s^{-1}$	Estimated from data in [40]
	40	$O_2^{\cdot-} + H^+ \rightarrow HO_2^{\cdot}a$	$10^5 s^{-1}$	Estimated from data in[40]
	41	$HO_2^{\cdot}a + HO_2^{\cdot}a \rightarrow H_2O_2 + O_2$	$7.6 \times 10^5\ M^{-1}s^{-1}$	[41]
	42	$HO_2^{\cdot}a + O_2^{\cdot-} + H^+ \rightarrow H_2O_2 + O_2$	$8.5 \times 10^7\ M^{-1}s^{-1}$	[41]
	43	$AscH^- + O_2 \rightarrow Asc^{\cdot-} + O_2^{\cdot-} + H^+$	$6 \times 10^{-4}\ M^{-1}s^{-1}$	[42]
3,4	44	$AscH^- + O_2^{\cdot-} + H^+ \rightarrow H_2O_2 + Asc^{\cdot-}$	$10^5\ M^{-1}s^{-1}$	Estimated from data in[43–46]
	45	$AscH^- + HO_2^{\cdot} \rightarrow H_2O_2 + Asc^{\cdot-}$	$1.2 \times 10^6\ M^{-1}s^{-1}$	[45]
	46	$Asc^{\cdot-} + O_2 \rightarrow Asc + O_2^{\cdot-}$	$6 \times 10^2\ M^{-1}s^{-1}$	[47]
	47	$Asc^{\cdot-} + O_2^{\cdot-} + 2H^+ \rightarrow Asc + H_2O_2$	$2.6 \times 10^8\ M^{-1}s^{-1}$	[48]
	48	$Asc^{\cdot-} + Asc^{\cdot-} + H^+ \rightarrow Asc + AscH^-$	$10^6\ M^{-1}s^{-1}$	[49]
	49	$Asc^{\cdot-} + HO_2^{\cdot} + H^+ \rightarrow Asc + H_2O_2$	$5 \times 10^9\ M^{-1}s^{-1}$	[48]
	50	$AscH^- + TocO^{\cdot} \rightarrow Asc^{\cdot-} + TocOH$	$2 \times 10^5\ M^{-1}s^{-1}$	[50]
	51	$HO_2^{\cdot}m + LH2 \rightarrow H_2O_2 + L^{\cdot}$	$1.18 \times 10^3\ M^{-1}s^{-1}$	[51]
	52	$HO_2^{\cdot}m + LH3 \rightarrow H_2O_2 + L^{\cdot}$	$1.7 \times 10^3\ M^{-1}s^{-1}$	[51]
	53	$HO_2^{\cdot}m + LH4 \rightarrow H_2O_2 + L^{\cdot}$	$3.05 \times 10^3\ M^{-1}s^{-1}$	[51]
	54	$HO_2^{\cdot}m + LH5 \rightarrow H_2O_2 + L^{\cdot}$	$6.7 \times 10^3\ M^{-1}s^{-1}$	Estimated from data in[51]
4	55	$HO_2^{\cdot}m + LH6 \rightarrow H_2O_2 + L^{\cdot}$	$1.6 \times 10^4\ M^{-1}s^{-1}$	Estimated from data in[51]
	56	$TocO^{\cdot} + O_2^{\cdot-} + H^+ \rightarrow O_2m + TocOH$	$4.5 \times 10^8\ M^{-1}s^{-1}$	[52]
	57	$TocOH + O_2^{\cdot-} + H^+ \rightarrow H_2O_2 + TocO^{\cdot}$	$6\ M^{-1}s^{-1}$	[53]
	58	$TocOH + HO_2^{\cdot}m \rightarrow H_2O_2 + TocO^{\cdot}$	$2 \times 10^5\ M^{-1}s^{-1}$	[53]
	59	$HO_2^{\cdot}m \rightarrow HO_2^{\cdot}a$	$10^{10}s^{-1}$	
	60	$HO_2^{\cdot}a \rightarrow HO_2^{\cdot}m$	$10^{10}s^{-1}$	
	61	$HO_2^{\cdot}m + HO_2^{\cdot}m \rightarrow H_2O_2 + O_2$	$7.6 \times 10^5\ M^{-1}s^{-1}$	[41]

	62	$Fe^{2+} + LOOH \rightarrow Fe^{3+} + LO^{\cdot} + HO^{-}$	$3.2 \times 10^2\ M^{-1}s^{-1}$	[55]
	63	$LH1 + LO^{\cdot} \rightarrow L^{\cdot} + LOH$	$3.8 \times 10^6\ M^{-1}s^{-1}$	Estimated from data in [56]
	64	$LH2 + LO^{\cdot} \rightarrow L^{\cdot} + LOH$	$8.8 \times 10^6\ M^{-1}s^{-1}$	Estimated from data in [56]
	65	$LH3 + LO^{\cdot} \rightarrow L^{\cdot} + LOH$	$1.3 \times 10^7\ M^{-1}s^{-1}$	Estimated from data in [56]
	66	$LH4 + LO^{\cdot} \rightarrow L^{\cdot} + LOH$	$2.05 \times 10^7\ M^{-1}s^{-1}$	Estimated from data in [56]
	67	$LH5 + LO^{\cdot} \rightarrow L^{\cdot} + LOH$	$3 \times 10^7\ M^{-1}s^{-1}$	Estimated from data in [56]
5	68	$LH6 + LO^{\cdot} \rightarrow L^{\cdot} + LOH$	$4 \times 10^7\ M^{-1}s^{-1}$	Estimated from data in [56]
	69	$LH1 + HO^{\cdot} \rightarrow L^{\cdot}$	$5 \times 10^8\ M^{-1}s^{-1}$	[57]
	70	$LH2 + HO^{\cdot} \rightarrow L^{\cdot}$	$5 \times 10^8\ M^{-1}s^{-1}$	[57]
	71	$LH3 + HO^{\cdot} \rightarrow L^{\cdot}$	$5 \times 10^8\ M^{-1}s^{-1}$	[57]
	72	$LH4 + HO^{\cdot} \rightarrow L^{\cdot}$	$5 \times 10^8\ M^{-1}s^{-1}$	[57]
	73	$LH5 + HO^{\cdot} \rightarrow L^{\cdot}$	$5 \times 10^8\ M^{-1}s^{-1}$	[57]
	74	$LH6 + HO^{\cdot} \rightarrow L^{\cdot}$	$5 \times 10^8\ M^{-1}s^{-1}$	[57]
	75	$LO^{\cdot} + TocOH \rightarrow TocO^{\cdot} + LOH$	$10^8\ M^{-1}s^{-1}$	Estimated from data in [21,58]
	76	$CatFe^{3+} + H_2O_2 \rightarrow Compound1$	$1.7 \times 10^7\ M^{-1}s^{-1}$	[59]
	77	$Compound1 + H_2O_2 \rightarrow CatFe^{3+} + O_2$	$2.6 \times 10^7\ M^{-1}s^{-1}$	[59]
6	78	$O_2^{\cdot-} + SODCu^{2+} \rightarrow O_2 + SODCu^{+}$	$1.9 \times 10^9\ M^{-1}s^{-1}$	Estimated from data in [60,61]
	79	$O_2^{\cdot-} + SODCu^{+} + 2H^{+} \rightarrow H_2O_2 + SODCu^{2+}$	$1.9 \times 10^9\ M^{-1}s^{-1}$	Estimated from data in [60,61]
	80	$HO^{\cdot} \rightarrow$	$2 \times 10^5 s^{-1}$	Estimated from data in [62-64]
	1a[b]	$LH1 + ROO^{\cdot} \rightarrow L^{\cdot} + ROOH$	$9 \times 10^{-3}\ M^{-1}s^{-1}$	Estimated from data in [21,27]
	2a[b]	$LH2 + ROO^{\cdot} \rightarrow L^{\cdot} + ROOH$	$18.05\ M^{-1}s^{-1}$	Estimated from data in [21]
	3a[b]	$LH3 + ROO^{\cdot} \rightarrow L^{\cdot} + ROOH$	$36.1\ M^{-1}s^{-1}$	Estimated from data in [21,27]
	4a[b]	$LH4 + ROO^{\cdot} \rightarrow L^{\cdot} + ROOH$	$54.15\ M^{-1}s^{-1}$	Estimated from data in [21,27]
7	5a[b]	$LH5 + ROO^{\cdot} \rightarrow L^{\cdot} + ROOH$	$72.2\ M^{-1}s^{-1}$	Estimated from data in [21,27]
	6a[b]	$LH6 + ROO^{\cdot} \rightarrow L^{\cdot} + ROOH$	$90.25\ M^{-1}s^{-1}$	Estimated from data in [21,27]
	81	$\rightarrow ROO^{\cdot}$	$10^{-9}\ Ms^{-1}$	
	82	$AscH^{-} + ROO^{\cdot} \rightarrow Asc^{\cdot-} + ROOH$	$10^5\ M^{-1}s^{-1}$	Estimated from data in [65]
	83	$O_2^{\cdot-} + ROO^{\cdot} \rightarrow O_2 + ROO^{-}$	$10^7\ M^{-1}s^{-1}$	Estimated from data in [41]
	84	$Asc^{\cdot-} + ROO^{\cdot-} \rightarrow Asc + ROO^{-}$	$10^9\ M^{-1}s^{-1}$	Estimated from data in [48]

[a] Adjusted in each case in order to mach the experimental rates of initiation.
[b] Reactions 1a through 6a account for the initiation in aqueous phase and replace reactions 1 through 6.

Mathematica[67] and C programs developed in our laboratory. The systems of differential equations were numerically integrated using algorithm LSODA[68], which is able to switch between a nonstiff (Adams') and a stiff (Gear's) method according to the behaviour of the integration process. (For methodological aspects of kinetic modelling of biochemical processes see [69]).

RESULTS

Basic reactional scheme of lipid peroxidation

The basic reactional scheme of lipid peroxidation was modelled considering model 1 (see Figure 1 and Table 1) with linoleoyl as the sole unsaturated fatty acyl chain. The peroxidation of lipid bilayers follows[70] the same limit law found in homogenous

TABLE 2
Kinetic orders of the rate of lipid peroxidation for several important parameters. The kinetic orders were calculated by observing the effect of changing each parameter on the maximal rate of peroxidation[a].

	Phase of initiation	R_i	LH	k_p	k_t
Experimental[70]	Aqueous	0.538 ± 0.016	1.07 ± 0.06	–	–
	Lipid	0.503 ± 0.032	1.05 ± 0.03	–	–
Simulated		0.500[b]	1.000	0.999[c]	−0.493[d]

[a] $k_2 = 5 \times 10^{-8}\ Ms^{-1}$; $[O_2]_m = 0.6$ mM; initial [LH2] = 2 M (other fatty acids are considered absent). [b] Calculated through systematic variation of k_2. [c] Calculated through systematic variation of k_{13}. [d] Calculated through systematic variation of k_{11}.

TABLE 3
Experimental conditions used in runs 21 and 22 of[71] and initial conditions used in simulations.

Run →		21 (Egg yolk)		22 (Rat liver)	
Initial conditions		Experimental	Simulation	Experimental	Simulation
Unsaturated fatty acyl chains	18:1 (LH1)	33.2%[a]	0.78 M[b]	27.6%[a]	0.65 M[b]
	18:2 (LH2)	15.8%[a]	0.37 M[b]	16.2%[a]	0.38 M[b]
	20:4 (LH4)	4.0%[a]	0.094 M[b]	6.2%[a]	0.15 M[b]
	22:5 (LH5)	0	0	1.3%[a]	0.03 M[b]
	22:6 (LH6)	0	0	2.4%[a]	0.06 M[b]
O_2 (membrane phase)		unknown[c]	0.6 mM[d]	unknown[c]	0.6 mM[d]
R_i (membrane phase)		1.8×10^{-6} Ms^{-1}[e]	1.8×10^{-6} Ms^{-1}[f]	3.6×10^{-6} Ms^{-1}[g]	3.6×10^{-6} Ms^{-1}[f]

[a] Molar fraction relative to all fatty acyl chains. [b] Estimate based on the composition of the liposomes and on a molar volume of 0.85 l/mol lipid[ref. 71]. [c] The oxidations were carried out under air at atmospheric pressure. [d] Kept constant in simulations. [e] Estimated from another run where the same amount of egg liposome and initiator was used. [f] The rate constants for initiation (k_1 through k_6) were assumed to follow the same relative proportions as those for propagation and have been adjusted in order to match the experimental R_i's. [g] Estimated from other runs with egg liposome.

solution: $-d[O_2]/dt = k_p [LH] R_i^{1/2}/(2 k_t)^{1/2}$. The kinetic orders observed in simulations are approximately those predicted by this law (Table 2).

The experiment[21] where the propagation and termination rate constants for autoxidation of dilinoleoylphosphatidylcholine (DLPC) bilayers were determined has also been simulated. The experimental and the simulated chain lengths agree within experimental reproducibility.

The oxidation of phosphatidylcholine multilamellar liposomes in aqueous dispersion was studied using azo compounds as initiators.[71] Since a mixture of unsaturated fatty acids is present, this experiment represents a more complex situation. Model 1 was used in this case too.

For the sake of simplicity, lipid radicals from different polyunsaturated fatty acyl chains were assumed to have similar chemical reactivity. The rate constants (k_{12} to k_{17}) for propagation have been estimated assuming that: a) $k_{13} = 18$ M^{-1}s^{-1} (linoleoyl fatty acyl chains)[21]; and b) the relative values (referred to k_{13}) of the other rate constants are 0.00057, 2.11, 2.65, 3.81, 4.97 for fatty acyl chains with 1, 3, 4, 5, and 6 double bonds, respectively. This series was estimated from data[27] for hydrogen abstraction from different acyl esters by tocopheroxyl radicals in homogeneous benzene solution. The rate constant for termination between peroxyl radicals was estimated from data[21] obtained for DLPC liposomes. The experimental conditions[71] and the corresponding initial conditions used in simulations are summarised in Table 3.

Overall, a satisfactory agreement was found between experimental and simulation results (Figure 2). The exception was linoleoyl in run 22. In face of the above mentioned agreement between simulations and experiments[21] using pure DLPC liposomes, it seems possible that other processes occurred during these experiments.[71] (E.g. changes in physical state of phospholipids.) It should also be stressed that the (low) consumption of linoleoyl was calculated[71] by difference between high amounts measured at the start of the experiment and at 60 minutes. It is thus likely to have a large margin of error. The estimates of the initial conditions (Table 3) were also less accurate than in the above reported simulations of the autoxidation of DPLC bilayers.

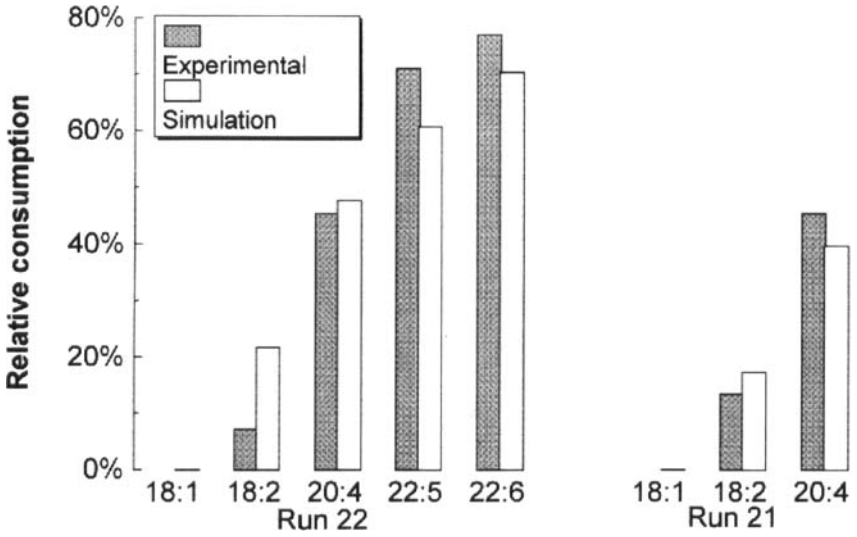

FIGURE 2 Comparison of the relative consumption of unsaturated fatty acyl chains observed experimentally[71] and in simulations. The percentages of fatty acid oxidised after 60 min relatively to the initial values are plotted. Initial conditions as in Table 3.

Antioxidant action of α-tocopherol

Barclay *et al.*[72] studied the oxidation of multilamellar DLPC liposomes using lipid-soluble and water-soluble initiators in presence of α-tocopherol. This experiment was simulated using model 2. The rate constant for reduction of peroxyl radical by α-tocopherol was determined[28] in DLPC liposomes. It is about two orders of magnitude lower than the values usually determined in homogeneous solution.[28] The initial conditions used in the simulations and the experimental conditions are indicated in Table 4.

The simulated time courses (Figure 3) of hydroperoxide accumulation and α-tocopherol consumption are similar to those usually found in experiments.

Theoretical (this work) and experimental[72] induction periods calculated in the same way agreed within about 10% (Figure 4). A better agreement (about 5%) was found

TABLE 4
Experimental conditions used in[72] and initial conditions used in the simulations.

Initial condition	Experimental	Simulation
Linoleoyl (LH2)	100%[a]	2 M[b]
O_2 (membrane phase)	unknown[c]	3 mM[d]

[a] Molar fraction relative to all fatty acyl chains. [b] Estimated from the composition and molar volume (1 l/mol lipid) of DLPC. [c] The results obtained by simulation are similar using oxygen either at atmospheric pressure or at 760 torr. [d] Kept constant in simulations.

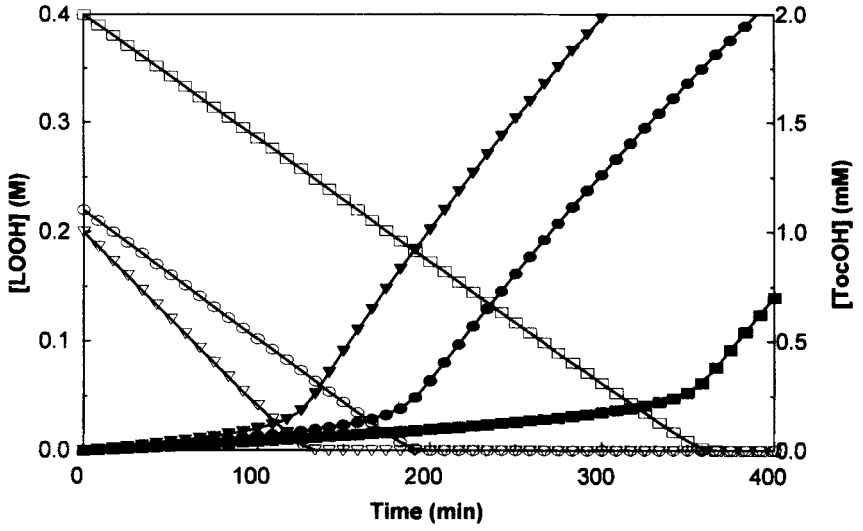

FIGURE 3 Simulated time course of runs 1 (squares), 2 (triangles) and 3 (circles) of[72]. Closed symbols, [LOOH]; open symbols, [TocOH]. Run 1, $R_i = 1.9 \times 10^{-7}$ Ms^{-1} and $[TocOH]_0 = 2.0$ mM; run 2, $R_i = 2.7 \times 10^{-7}$ Ms^{-1} and $[TocOH]_0 = 1.0$ mM; run 3, $R_i = 2.0 \times 10^{-7}$ Ms^{-1} and $[TocOH]_0 = 1.1$ mM. Rates and concentrations referred to membrane phase. Other initial conditions as in Table 4.

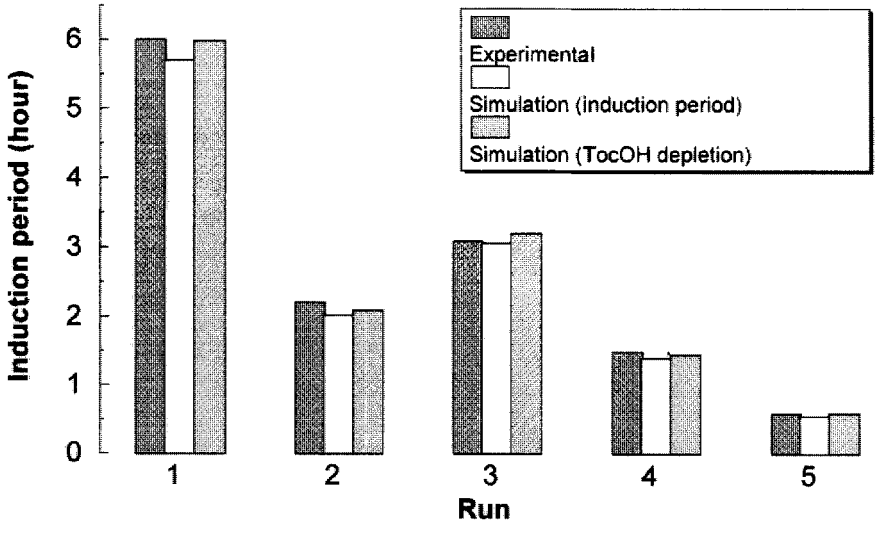

FIGURE 4 Comparison of the induction period obtained experimentally[72] and from simulations. TocOH depletion indicates the time necessary to reach 'complete' oxidation of α-tocopherol. Run 1, 2, and 3 as in Figure 3; run 4, $R_i = 5.4 \times 10^{-7}$ Ms^{-1} and $[TocOH]_0 = 1.4$ mM; run 5, $R_i = 4.9 \times 10^{-7}$ Ms^{-1} and $[TocOH]_0 = 0.51$ mM. Rates and concentrations referred to membrane phase. Other initial conditions as in Table 4.

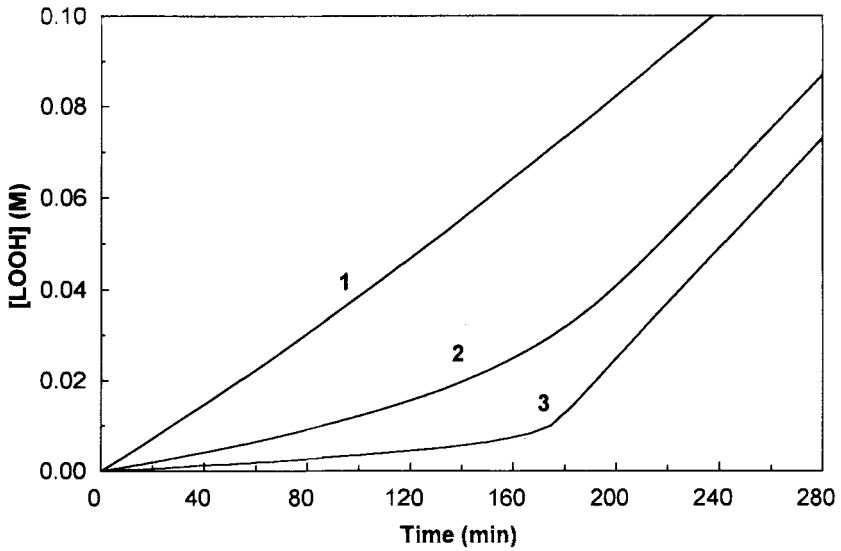

FIGURE 5 Time course of DLPC oxidation in presence of hypothetical chain breaking antioxidants with different activities. Simulated with the initial conditions in Table 4 and $R_i = 1.67 \times 10^{-8}$ Ms^{-1}, $[antioxidant]_0 = 0.0875$ mM. 1, $k_{18} = 5.8 \times 10^2 M^{-1}s^{-1}$; 2, $k_{18} = 5.8 \times 10^3 M^{-1}s^{-1}$ (α-tocopherol); 3, $k_{18} = 5.8 \times 10^4 M^{-1}s^{-1}$.

when we compared the experimental induction period with the time (τ) necessary to reach 'complete' oxidation of α-tocopherol* in simulations. Since the rate of initiation used in simulations was estimated from induction periods using the expression $R_i = 2[TocOH]/\tau$, this is not surprising.

As observed experimentally,[73] the simulated induction periods are independent of the local concentration of fatty acyl moieties. They are best defined for chain breaking antioxidants able to reduce lipid peroxyl radicals with high rate constants (Figure 5), provided the rate constants of the other reactions are unchanged. This feature is also found in experiments.

Liebler *et al.*[74] studied the oxidation of multilamellar liposomes of soybean phospholipids in presence of α-tocopherol. The oxidant system was 0.1 mM Fe^{2+} (as $Fe(NH_4)_2(SO_4)_2$)/0.1 mM H_2O_2. The mechanisms of action of iron on the peroxidation of phospholipid membranes are not very well understood. However, we could estimate the rate of initiation in[74] from the induction periods caused by α-tocopherol. Hence, initiation was assumed to proceed through hydrogen abstraction from the unsaturated fatty acyl chains at the experimental rate, and no reactions of iron were explicitly considered. Therefore model 2 was used. The initial conditions used in simulation and the experimental conditions[74] are indicated in Table 5.

Liebler *et al.*[74] plotted the concentration of thiobarbituric acid reactive substances (TBARS) – used as an indicator of the rate of peroxidation – against [TocOH] at several

*Calculated as the time of intersection between the horizontal axis ([TocOH] = 0) and the tangent to the plot of α-tocopherol consumption at the phase of maximal consumption.

TABLE 5
Experimental conditions used in [74] and initial conditions used in the simulations.

Initial condition		Experimental	Simulation
Unsaturated	18:1 (LH1)	11.2%[a,b]	0.26 M[c]
fatty acyl	18:2 (LH2)	67.3%[a,b]	1.56 M[c]
chains	18:3 (LH3)	5.9%[a,b]	0.14 M[c]
O_2 (membrane phase)		unknown[d]	0.6 mM[e]
α-tocopherol		several concentrations	20 mM
Fe^{2+}		0.1 mM	0[f]
H_2O_2		0.1 mM	0[f]
R_i (membrane phase)		unknown[g]	$2 \times 10^{-4} Ms^{-1}$ ($k_1 = k_2 = k_3 = 10^{-4} s^{-1}$)

[a] Molar fraction relative to all fatty acyl chains. [b] The composition of the liposomes is not referred in [74]. Data from [71] are used instead. [c] Calculated from the composition of soybean liposomes using a molar volume of 0.86 l/mol lipid[ref. 71]. [d] The oxidations were carried out under air at atmospheric pressure. [e] Kept constant in simulations. [f] The pro-oxidant system was replaced by an hypothetical initiator. [g] An $R_i \approx 2 \times 10^{-4} Ms^{-1}$ can be estimated from an experiment studying the effect of α-tocopherol on the time delay to achieve maximal oxygen consumption.

incubation times. In Figure 6 the rates of hydroperoxide production obtained in simulations are plotted along these experimental data. Provided TBARS are directly proportional to the rate of hydroperoxide production, a good qualitative agreement is found. A quantitative agreement cannot be evaluated, as the conversion of TBARS into rate of lipid peroxidation is not known.

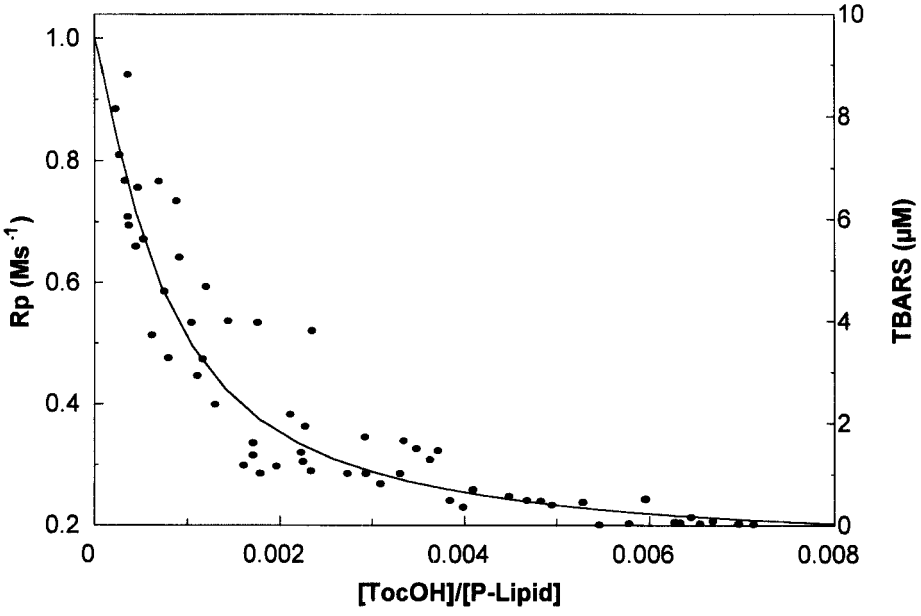

FIGURE 6 Dependence of the rate of LOOH production on α-tocopherol concentration. Theoretical (line) and experimental[74] results (dots) are compared. Rates of peroxidation (R_p) obtained in simulation or thiobarbituric acid reactive substances (TBARS) measured in experiments during the oxidation of soybean liposomes are plotted against the levels of α-tocopherol found at the corresponding times.

TABLE 6
Experimental conditions used in[75] and corresponding initial conditions used in simulation.

Initial conditions	Experimental	Simulation
O_2 (aqueous phase)	unknown[a]	0.2 mM[b]
Catalase (SOD free)	2×10^{-7} M	2×10^{-7}M
pH	7.4	7.4[c]

[a] The oxidation procedures were carried out under air at atmospheric pressure. [b] Kept constant in simulations. [c] The values for k_{39}, k_{40} and k_{48} shown in Table 1 were adjusted for this pH.

Antioxidant action of ascorbate

Since the autoxidation of ascorbate in aqueous phase can influence significantly its protective action against the peroxidation of lipid membranes, we will analyse the former process first. Scarpa *et al.*[75] studied the autoxidation of ascorbate in presence of iron, superoxide dismutase and catalase. Model 3 was used in simulations of this experiment. The experimental conditions and the initial conditions used in the simulations are indicated in Table 6.

The effect of different concentrations of SOD on the rate of ascorbate oxidation is plotted in Figure 7. Further results are compared in Table 7. A good agreement has been found between experimental and simulated ratios of rates. Simulations and experiments[75] further agreed in that the steady-state concentration of semi-

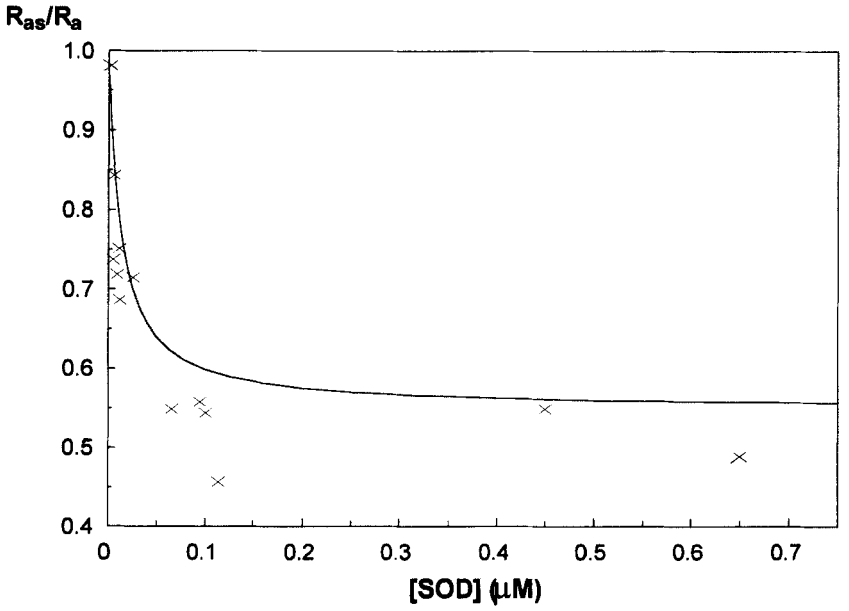

FIGURE 7 Effect of the concentration of SOD on the initial rate of ascorbate oxidation. Theoretical (line) and experimental[75] (X) results are compared. $[AscH^-] = 1.2 \times 10^{-4}$ M; $[Fe^{3+}\text{-EDTA}] = 4.7 \times 10^{-6}$ M. In the simulation the rate of ascorbate oxidation was averaged over the range 10 s – 40 s. R_a, R_{as}: rate of ascorbate oxidation in absence and in presence of SOD, respectively.

TABLE 7
Experimental[75] and simulated rates and ratios of superoxide generation and ascorbate oxidation. [AscH$^-$] = 7.6×10^{-5} M; [Fe^{2+} – EDTA] = 3×10^{-6} M. R_{os}, R_{as}, Initial rates of superoxide generation and of ascorbate oxidation, respectively, in presence of a saturating concentration (2×10^{-6} M) of SOD. R_o, R_a, Rates in absence of SOD.

	$R_{os}{}^a(Ms^{-1})$	$R_{os}{}^b(Ms^{-1})$	$R_o{}^b(Ms^{-1})$	$R_o{}^b/R_a{}^b$	$R_{os}{}^a/R_a{}^b$	$R_a{}^b/R_{as}{}^b$
Experimental[75]	4.90×10^{-8}	–	–	–	1.01	1.91
	5.40×10^{-8}	–	–	–	1.03	1.98
Simulation	1.46×10^{-7}	1.43×10^{-7}	1.64×10^{-7}	1.26	1.12	1.92

[a] Calculated from the time necessary for SOD to reach steady-state as characterised by $[Cu^{2+}]/[Cu^+] = 1$. The theoretical model supports this as a good approximation (see second column of data).[b] Averaged over the range 10 s–40 s.

dehydroascorbate is fairly independent of the experimental conditions. However, the absolute fluxes of $O_2^{\cdot-}$ generation and of ascorbate oxidation were approximately three times higher in the simulations, and while the concentration of semidehydroascorbate has been reported[75] to increase by about 20% upon addition of $>10^{-7}$ M SOD, the simulations predicted a decrease of about 37%.

The simulations indicated that the autoxidation of ascorbate in presence of SOD is mainly influenced by reactions 28, 36, and 38. In absence of SOD, reaction 44 is also important. Since the rate of the latter reaction was similar to that of ascorbate oxidation by ferric ion, the effect of saturating the system with SOD was halving the total rate of ascorbate oxidation, as observed both in experiments[75] and in simulations (Figure 7).

The rate constant for reaction 36 was guessed by comparison to other similar reactions as, to our knowledge, it has never been measured. Furthermore, the formation and actions of possible ferryl species was not taken into account, due to the lack of quantitative kinetic data. Altogether, these facts may explain the discrepancies mentioned above.

A study of the antioxidant activity of ascorbate against the peroxidation of aqueous multilamellar DLPC liposomes in presence of α-tocopherol was reported.[76] Lipid peroxidation was initiated by a lipid-soluble initiator. This experiment was simulated using model 4. The experimental conditions[76] and the initial conditions used in simulations are indicated (Table 8).

TABLE 8
Experimental conditions used in [76] and corresponding initial conditions used in simulation.

Initial conditions	Experimental	Simulation
Linoleoyl (LH2)	100%[a]	2 M
O_2 (aqueous phase)	unknown[b]	1 mM[c]
O_2 (membrane phase)	unknown[b]	3 mM[c]
α-tocopherol	0.66 mM	0.66 mM
Ascorbate	53.5 μM[d]	53.5μM[e]
Fe^{2+}	unknown[f]	0[f]
R_i (membrane phase)	$7 \times 10^{-8} Ms^{-1}$[g]	$7 \times 10^{-8}\ Ms^{-1}$ ($k_2 = 3.5 \times 10^{-8} s^{-1}$)
pH	7	7[h]
Vol. aqueous phase/vol. membrane phase	62[i]	62

[a] Molar fraction relative to all fatty acyl chains. [b] The oxidation procedures were carried out under 760 torr oxygen. [c] Kept constant in simulations. [d] Referred to total reactional volume. [e] Referred to aqueous phase. [f] The buffer was passed through a column of Chelex 100[76]. [g] Estimated from the induction period induced by α-tocopherol. [h] The values for k_{39}, k_{40} and k_{48} were readjusted for this pH ($2 \times 10^7 s^{-1}$, $10^5 s^{-1}$ and $2 \times 10^6 M^{-1}s^{-1}$, and $2 \times 10^6 M^{-1}s^{-1}$, respectively). [i] Estimated from the molar volume of DLPC (1 l/mol lipid).

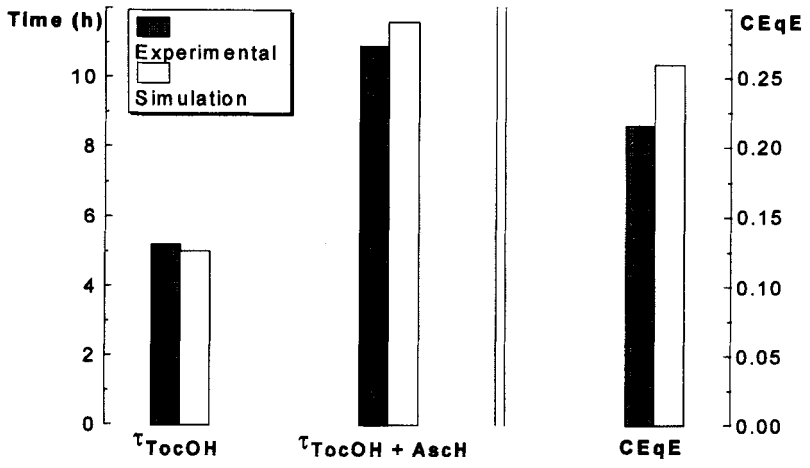

FIGURE 8 Antioxidant effect of ascorbate on DLPC liposomes. Comparison between experimental[76] and simulation results. τ_{TocOH}, induction period induced by α-tocopherol; $\tau_{TocOH+AscH}$, induction period induced by α-tocopherol plus ascorbate; CEqE, number of molecules of α-tocopherol spared by one molecule of ascorbate, calculated as $[(\tau_{TocOH+AscH} - \tau_{TocOH})/n_{AscH}]/(\tau_{TocOH}/n_{TocOH})$.

Experimental and simulated induction periods showed good agreement (Figure 8).

The time courses of ascorbate, α-tocopherol, semidehydroascorbate and α-tocopheroxyl concentrations (Figure 9) were similar to those observed in most experiments:[50,77,78] significant rates of α-tocopherol oxidation are only observed after total oxidation of ascorbate.

In some experiments using *multilamellar* liposomes – see Figure 4 of Niki *et al.*[77] and Figure 2 of Doba *et al.*[76] – a significant rate of α-tocopherol oxidation has been observed before ascorbate was completely oxidised. In the latter work[76] a rapid consumption of α-tocopherol was followed by a period during which α-tocopherol was spared before being again rapidly oxidised. These unusual behaviours are not explained in[76,77]. We suggest that they may be due to the inability of ascorbate to reduce α-tocopheroxyl in the inner layers of the liposomes. This hypothesis was tested using model 5, a modification of model 4 with two lipid compartments. The first was in contact with the aqueous phase, while the second was isolated from both the aqueous phase and the other lipid compartment. The lipid compartments were assumed to have the same initial composition and rate of initiation and to undergo the same reactions except for the lipid-water interface reactions (reactions 50, 56, 57, 59, 60 in Table 1), which only involve one of them. In curve 1 (Figure 10), the situation is identical to that described in Figure 9. When – curve 2 – 20% of the lipid phase was isolated from the aqueous phase, simulation results were similar to those of Niki *et al.*[77]. The results reported by Doba *et al.*[76] have been simulated – curve 3 – assuming that 50% of the lipid phase was accessible to molecules in the aqueous phase.

The hypothesis can be tested experimentally by systematic observation of how the time course of α-tocopherol oxidation depends on the proportion of lipid phase accessible from the aqueous phase: assuming that the lipid compartments do not

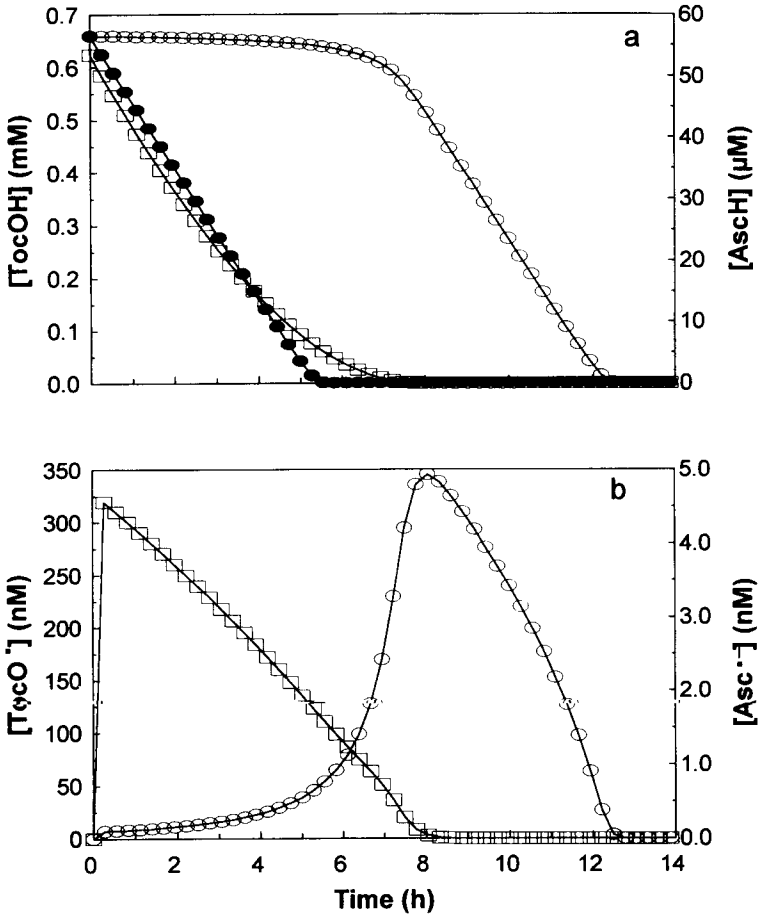

FIGURE 9 Simulated time course of α-tocopherol consumption during the autoxidation of DLPC liposomes in presence (open symbols) and in absence (closed symbols) of ascorbate. The initial conditions used in the simulation are shown in Table 8. a) Circles, α-tocopherol; squares, ascorbate monoanion. b) Circles, α-tocopheroxyl radical; squares, semidehydroascorbate.

significantly exchange any forms of lipid nor α-tocopherol during the experiments, the time courses of α-tocopherol and lipid hydroperoxide concentrations should appear as presented in Figure 11.

Wayner *et al.*[79] and Pryor *et al.*[65] have also studied the antioxidant action of ascorbate using different experimental systems. The former workers[79] reported the number (n) of peroxyl radicals trapped by each ascorbate molecule to approach 2 as ascorbate concentration decreased, and to approach nil as ascorbate concentration increased.[79] They did not observe a dependence of n on oxygen concentration, in contrast to the findings of Pryor *et al.*[65] In order to investigate this issue theoretically, we studied the dependence of n on ascorbate concentration under three different concentrations of oxygen and iron, in two different systems. In the first system (model 6), the initiator was assumed to be present exclusively in lipid phase, allowing ascorbate to regenerate α-tocopherol from its radical but not to trap peroxyl radicals originated

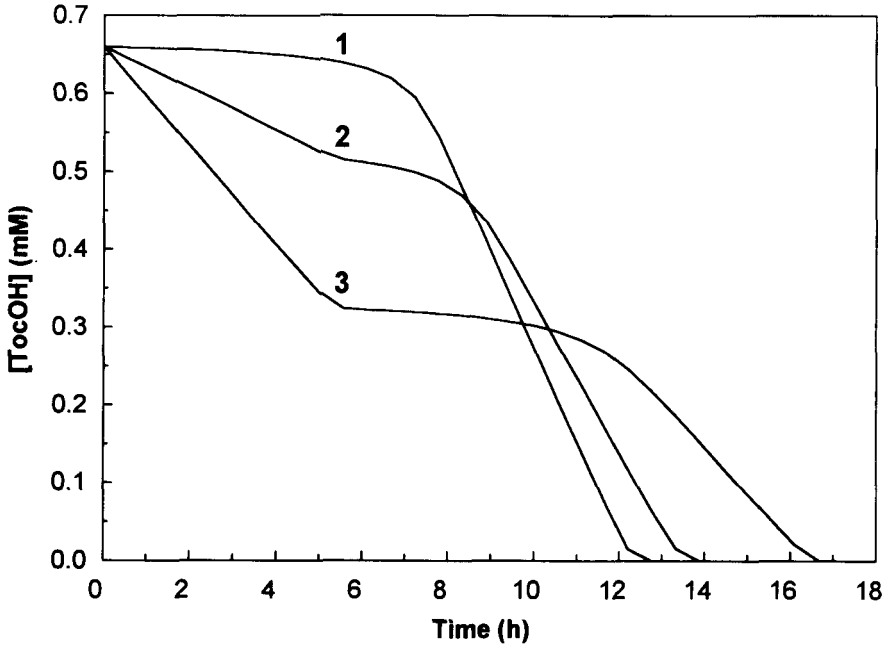

FIGURE 10 Effect of the accessibility of ascorbate to the lipid phase on the sparing of α-tocopherol: 1, ascorbate has access to all lipid phase; 2, ascorbate has access to 80% of the lipid phase; 3, ascorbate has access to 50% of the lipid phase.

directly from the initiator. The same conditions as in the simulation of the experiment in Doba *et al.*[76] were used in this case. In the second system (model 7), the initiator was assumed to be present exclusively in the aqueous phase, allowing ascorbate to trap peroxyl radicals originated directly from the initiator and to regenerate α-tocopherol. The effects of reactions 51–58, 62 and 69–74 on the concentration of the lipid-soluble species were discarded, thus allowing the effects of different oxygen and iron concentrations on the efficiency of ascorbate to be directly compared. Results are presented in Figure 12. The main observations were:

a) n decreases as the concentration of iron increases. This is due to the iron-catalysed autoxidation of ascorbate.
b) The presence of 0.1–0.5 μM iron decreases the dependence (in absolute terms) of n on oxygen concentration (compare plots a, b, c and d, e, f in Figure 12).
c) n is lower in the system with initiation in lipid phase than in the system with initiation in aqueous phase, since ascorbate is able to scavenge peroxyl radicals only in aqueous phase.
d) In the case of *initiation in aqueous phase* without iron at low O_2 and ascorbate concentrations, values of n higher than 2 were observed (Figure 12a, curve 1). In this system one molecule of ascorbate can regenerate one molecule of α-tocopherol, which traps two peroxyl radicals and forms one molecule of semi-dehidroascorbate. The latter molecule can trap one peroxyl in aqueous phase.

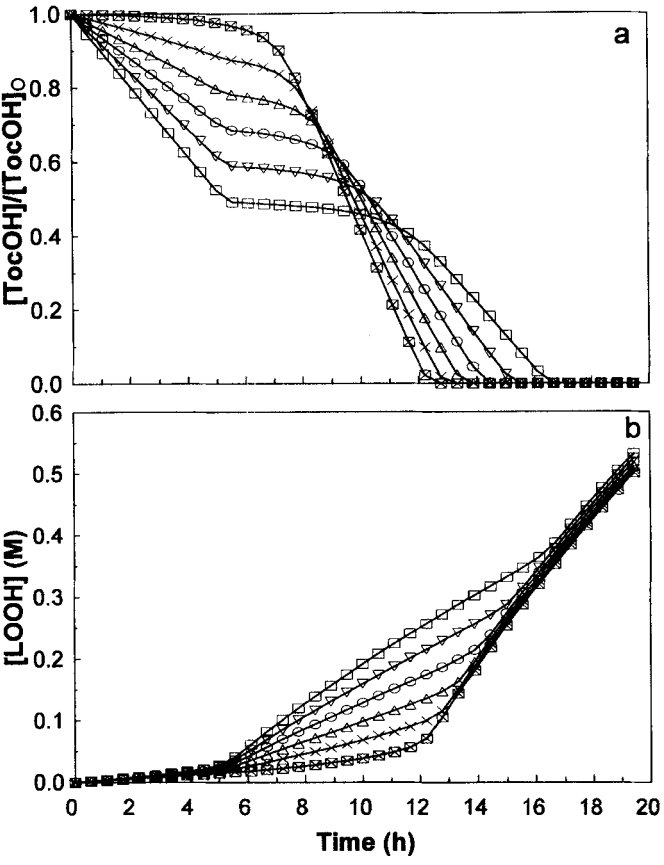

FIGURE 11 Simulated time courses of α-tocopherol consumption (a) and hydroperoxide production (b) for different proportions of lipid phase accessible from the aqueous phase. ⊠, 100%; ×, 90% Δ, 80%; m , 70%; ∇, 60%; o , 50%.

Therefore, values of n as high as 3 are theoretically possible.† However, most ascorbate molecules will react with peroxyl radicals in aqueous phase, leading to n near 2 under low rates of autoxidation.

e) In the case of *initiation in lipid phase* at low O_2 and ascorbate concentrations in absence of iron, n increases with ascorbate concentration (Figure 12d, curve 1). Simulations suggest a possible explanation. If ascorbate is not plentifully available for α-tocopherol regeneration (reaction 50) unsaturated fatty acyl chains may compete significantly (through reaction 20) with ascorbate for the α-tocopheroxyl radicals.

f) Other experimental conditions found to affect ascorbate efficiency as antioxidant are the rate of initiation of lipid peroxidation in lipid phase (higher rates lead to higher n) and the volume ratio of aqueous to lipid phase (lower ratios increase n).

†Even higher values would be possible if semidehydroascorbate reacted with oxygen forming superoxide radical, which, in a hypothetical interface reaction, could regenerate α-tocopherol.

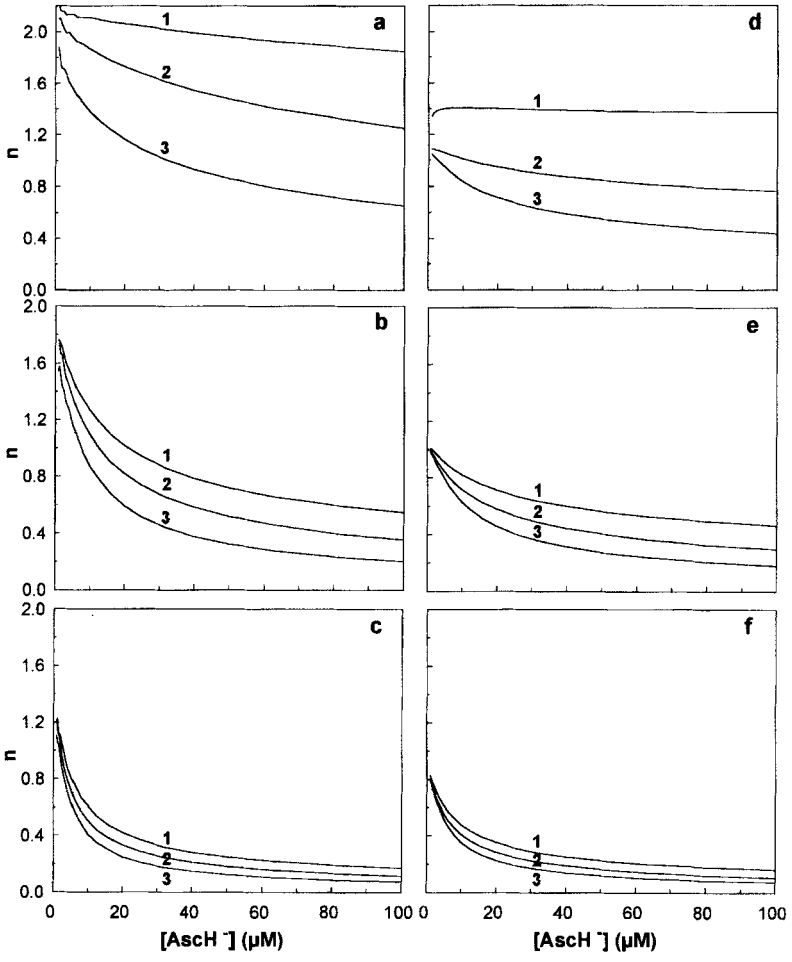

FIGURE 12 Influence of ascorbate concentration on the number (n) of peroxyl radicals trapped per ascorbate molecule. a), b) and c): initiation in aqueous phase; d), e) and f): initiation in lipid phase. a) and d): without iron; b) and e): $[Fe^{2+}]_0 = 0.1$ μM; c) and f): $[Fe^{2+}]_0 = 0.5$ μM; 1, $[O_2]_{aq} = 0.04$ mM, $[O_2]_m = 0.12$ mM; 2, $[O_2]_{aq} = 0.2$ mM, $[O_2]_m$ 0.6 mM; 3, $[O_2]_{aq} = 1$ mM, $[O_2]_m$ =3 mM. n is calculated as twice the value of CEqE (see legend of Figure 8).

These results suggest that the efficiency of ascorbate as antioxidant is strongly dependent on experimental conditions such as the amount of iron in the system. Apparently contradictory results[79,65] as those referred above seem to be explained by this dependency. Namely, the system used by Wayner *et al.* did contain iron,[79] while probably no significant amounts of iron were present in the system used by Pryor *et al.*[65]

DISCUSSION

Overall, the results show the possibility of formulating kinetic models that are able to simulate *in vitro* lipid peroxidation experiments with different degrees of complexity. Quantitative to semiquantitative agreement was found between simulations and experimental results. The analysis of the models suggested, in addition, new hypotheses and experiments. It also points out some aspects of lipid peroxidation requiring further investigation:

- Simulations of model 1 support the current perception that the time course of the non-inhibited lipid peroxidation is mainly influenced by the rate constants for propagation (k_{12}–k_{17}) and for termination between two peroxyl radicals (k_{11}). These absolute rate constants determined in DLPC liposomes differ significantly from those determined in micelles or in homogeneous solutions.[21,80] Unfortunately, liposome data regarding the other biologically important unsaturated fatty acyl chains are still missing. The knowledge of such important rate constants would, in principle, allow a more accurate simulation of lipid peroxidation in biological membranes.
- Analysis of model 4 and other related models indicates (Salvador, Antunes and Pinto, paper in preparation) that the synergism between ascorbate and α-tocopherol is strongly dependent on the rate constants for regeneration of $TocO^{\bullet}$ by $AscH^{-}$ (reaction 50) and for the reaction between $TocO^{\bullet}$ and $LOO^{\bullet}$ (reaction 25). Both rate constants have a large margin of uncertainty. Given the probable biological importance of these reactions, it would be of interest to obtain accurate determinations in liposomes.
- The proteins in biomembranes may significantly influence the dynamics of lipid peroxidation. Few studies about this matter were found suitable for simulation. Simulations assuming a passive role for proteins were made using model 2 with the concentrations of all lipid species corrected by a dilution factor. After matching the initial conditions the induction periods agreed with those found in experiments[81] on oxidation of erythrocyte ghost membranes. Yet, the experimental chain lengths were ≈ 50% lower than predicted. The precision and degree of control of these experiments do not allow to ascertain the significance of this discrepancy. However, it may suggest that proteins did play an active role in the peroxidation of membrane lipids. Better controlled experiments, using membranes of precisely known composition, seem necessary to elucidate this issue.
- The lack of quantitative knowledge about the basic redox chemistry of iron also represents a significant difficulty in modelling some aspects of oxidative stress. Although the simple set of reactions presented in modules 3 and 5 accounts for some known effects of that transition metal, we are aware that it is a most sketchy model of a far more complex process.

Theoretical-experimental approaches combining the use of kinetic models with quantitative experiments appear promising in the study of oxidative stress. However, for such approaches to be successful, an increased effort has to be dedicated to quantification and to control of environmental variables. Simple and well-defined experimental systems will probably be the most informative, especially if they can reproduce the physico-chemical conditions prevailing in biological environments.

One of the main goals of this work is to support the use of moderately detailed kinetic models of in vivo *lipid peroxidation.* Indeed, the ability to simulate relatively complex

reactional systems at a semiquantitative level encourages integrating the reactional schemes used above into such a model (see[19]). In doing so, it must be kept in mind that the cellular environment is complex and very different from the conditions prevailing *in vitro* during kinetic determinations. *Such modelling must, therefore, be aimed predominantly at understanding qualitative aspects, although it may provide order-of-magnitude estimates for variables that are difficult to measure experimentally, such as the concentrations of some radicals.*

One particularly important way in which usual *in vitro* experiments differ from biological systems is that the latter are open systems. If unperturbed, the former will approach thermodynamic equilibrium and any net changes will vanish, while the latter will approach some kind of long term behaviour. (E.g. a steady state, where concentrations no longer change in spite of the occurrence of net fluxes in the system). Both the formulation and the analysis of the models have to reflect that difference. Thus, models of *in vivo* phenomena must take into account the influxes into and effluxes from the system. Furthermore, while the theoretical analyses described in this paper concentrated on studying transient phenomena, the analysis of models of 'intact' biochemical systems is usually centred in the study of the long term behaviour. This is dictated both by mathematical convenience and by a common wisdom that metabolic processes normally stay around that long term behaviour.

In addition to a systematic 'low level' validation, an 'high level' validation should be performed by testing the ability of the model to predict a suitable set of known physiological responses. Ideally, a set of specially designed experiments should be planned to maximise both the efficiency and the robustness of the validations.

Finally, whatever the success of a model in passing validations, the true measure of its value is its usefulness as a tool for improving knowledge of oxidative stress.

Acknowledgements

We are grateful to Professor L.R.C. Barclay for helpful discussions and to Susana Marinho for helpful discussions and careful revision of the manuscript. A.S. and F.A. acknowledge support from grants BD/146/90-RM ('Programa CIENCIA'/JNICT) and FMRH-BD-399–92/JNICT, respectively. IICBRC and JNICT (FACC) contribute to the support of GBBT.

References

1. Y.A. Vladimirov, P.I. Gutenev and P.I. Kuznetsov (1973) Mathematical modelling of chain oxidation kinetics of biopolymembrane lipids in the presence of ions. *Biofizika*, **18,** 1024–1030 (in Russian).
2. Y.A. Vladimirov and Y.M. Petrenko (1976) Determination of antioxidants action mechanisms in lipid systems according to chemoluminescence parameters in the presence of ferrous oxide. *Biofizika*, **21,** 424–427 (in Russian).
3. D.S. Chernavskii, E.K. Palamarchuk, A.A. Polezhaev, G.I. Solyanik and E.B. Burlakova (1977) A mathematical model of periodic processes in membranes (with application to cell cycle regulation). *Biosystems*, **9,** 187–193.
4. Y.A. Vladimirov, V.I. Olenev, T.B. Suslova and Z.P. Cheremisina (1980) Lipid peroxidation in mitochondrial membrane. *Advances in Lipid Research*, **17,** 173–249.
5. E.I. Volkov (1987) Mathematical model of the kinetics of lipid peroxidation. *Khimicheskaya Fizika*, **6,** 361–368 (in Russian).
6. K. Schwetlick (1988) Inhibition kinetics of initiated autoxidations. *Journal of Chemical Society. Perkin Transactions II*, 2007–2010.
7. A.E. Sitnitsky and E.I. Volkov (1989) Oxygen relationship of the kinetics of unenzymic peroxidation of lipids. *Biofizika*, **34,** 230–234 (in Russian).
8. C. Babbs and M.G. Steiner (1990) Simulation of free radical reactions in biology and medicine: a new two-compartment kinetic model of intracellular lipid peroxidation. *Free Radical Biology and Medicine*, **8,** 471–485.
9. A.A. Remorova and V.A. Roginskii (1991) Rate constants for the reaction of α-tocopherol phenoxy

radicals with unsaturated fatty acid esters, and the contribution of this reaction to the kinetics of inhibition of lipid peroxidation. *Kinetics and Catalysis*, **32,** 726–731.
10. V.A. Roginski and I.V. Utkin (1991) Kinetics of autoxidation of unsaturated fatty acid esters. *Kinetics and Catalysis*, **32,** 732–737.
11. J. Remacle, D. Lambert, M. Raes, E. Pigeolet, C. Michiels and O. Toussaint (1992) Importance of various antioxidant enzymes for cell stability – Confrontation between theoretical and experimental data. *Biochemical Journal*, **286,** 41–46.
12. A. Salvador, F. Antunes and R.E. Pinto (1993) Simulation and analysis of a complex biochemical process: lipid peroxidation in inner mitochondrial membranes. In *Proceedings of the 1st Copenhagen Symposium on Computer Simulation in Biology, Ecology and Medicine* (ed. E. Mosekilde), Simulation Councils Inc., San Diego, pp. 69–73.
13. V.W. Bowry and R. Stocker (1993) Tocopherol-mediated peroxidation. The prooxidant effect of vitamin E on the radical-initiated oxidation of human low-density lipoprotein. *Journal of American Chemical Society*, **115,** 6029–6044.
14. P. Moniz-Barreto and D.A. Fell (1993) Simulation of dioxygen free radical reactions. *Biochemical Society Transactions*, **21,** 256S.
15. A. Kowald and T.B.L. Kirkwood (1994) Towards a network theory of ageing: a model combining the free radical theory and the protein error theory. *Journal of theoretical Biology*, **168,** 75–94.
16. Y.J. Suzuki and G.D. Ford (1994) Mathematical model supporting the superoxide theory of oxygen toxicity. *Free Radical Biology and Medicine*, **16,** 63–72.
17. J.I.S. MacDonald and H. Sprecher (1991) Phospholipid fatty acid remodelling in mammalian cells. *Biochimica Biophysica Acta*, **1084,** 105–121.
18. D.R. Voelker (1991) Organelle biogenesis and intracellular lipid transport in eukaryotes. *Microbiological Reviews*, **55,** 543–560.
19. F. Antunes, A. Salvador, H.S. Marinho and R.E. Pinto (1994) A mathematical model for lipid peroxidation in inner mitochondrial membranes. *Travaux de Laboratoire*, **XXXIV** suppl. T-I., Instituto de Investigação Científica Bento da Rocha Cabral, Lisbon. (Available upon request to the authors).
20. W.K. Subczynski and J.S. Hyde (1983) Concentration of oxygen in lipid bilayers using a spinlabel method. *Biophysical Journal*, **41,** 283–286.
21. L.R.C. Barclay, K.A. Baskin, S.J. Locke and M.R. Vinqvist (1989) Absolute rate constants for lipid peroxidation and inhibition in model biomembranes. *Canadian Journal of Chemistry*, **67,** 1366–1369.
22. L.K. Patterson and K. Hasegawa (1978) Pulse radiolysis studies in model lipid systems: The influence of aggregation on kinetic behavior of OH induced radicals in aqueous sodium linoleate. *Berichte der Bunsengesellschaft fur Physikalische Chemie*, **82,** 951–956.
23. K. Hasegawa and L.K. Patterson (1978) Pulse radiolysis studies in model lipid systems: formation and behaviour of peroxy radicals in fatty acids. *Photochemistry and Photobiology*, **28,** 817–823.
24. W. Bors, M. Erben-Russ, and M. Saran (1987) Fatty acid peroxyl radicals: their generation and reactivities. *Bioelectrochemistry and Bioenergetics*, **18,** 37–49.
25. N.A. Porter, L.S. Lehman, B.A. Weber and K.J. Smith (1981) Unified mechanism for polyunsaturated fatty acid autoxidation. Competition of peroxy radical hydrogen atom abstraction, β-scission, and cyclization. *Journal of the American Chemical Society*, **103,** 6447–6455.
26. N. Uri (1961) Physico-chemical aspects of autoxidation. In *Autoxidation and antioxidants*, (ed. W.O. Lundberg), Wiley-Interscience, New York, pp. 55–106. (Referred in [8])
27. S. Nagaoka, Y. Okauchi, S. Urano, U. Nagashima and K. Mukai (1990) Kinetic and ab initio study of the prooxidant effect of vitamin E. Hydrogen abstraction from fatty acid esters and egg yolk lecithin. *Journal of the American Chemical Society*, **112,** 8921–8924.
28. L.R.C. Barclay, K.A. Baskin, K.A. Dakin, S.J. Locke and M.R. Vinqvist (1990) The antioxidant activities of phenolic antioxidants in free radical peroxidation of phospholipid membranes. *Canadian Journal of Chemistry*, **68,** 2258–2269.
29. A.A. Remorova and V.A. Roginskii (1991) Rate constants for the reaction of α-tocopherol phenoxy radicals with unsaturated fatty acid esters, and the contribution of this reaction to the kinetics of inhibition of lipid peroxidation. *Kinetics and Catalysis*, **32,** 726–731.
30. M.N. Kaouadji, D. Jore, C. Ferradini and L.K. Patterson (1987) Radiolytic scanning of vitamin E-vitamin C oxidation-reduction mechanisms. *Bioelectrochemistry and Bioenergetics*, **18,** 59–70.
31. K. Mukai, Y. Kohno and K. Ishizu (1988) Kinetic study of the reaction between vitamin E radical and alkyl hydroperoxides. *Biochemical and Biophysical Research Communications*, **155,** 1046–1050.
32. C. Bull, G.J. McClune and J.A. Fee (1983) The mechanism of Fe-EDTA catalysed superoxide dismutation. *Journal of the American Chemical Society*, **105,** 5290–5300.
33. Z. Stuglik and Z.P. Zagorski (1981) Pulse radiolysis of neutral iron(II) solutions: Oxidation of ferrous ions by OH radicals. *Radiation Physics and Chemistry*, **17,** 229–233.

34. H.A. Schwarz (1962) A determination of some rate constants for the radical processes in the radiation chemistry of water. *Journal of Physical Chemistry*, **66,** 255–262.
35. J.K. Thomas (1965) Rates of reaction of the hydroxyl radical. *Transactions of the Faraday Society*, **61,** 702–707.
36. K. Sehested, O.L. Rasmussen and H. Fricke (1968) Rate constants of OH with O_2^-, and $H_2O_2^+$ from hydrogen peroxide formation in pulse-irradiated oxygenated water. *Journal of Physical Chemistry*, **72,** 626–631.
37. J.D. Rush and B.H.J. Bielski (1985) Pulse radiolytic of the reactions of HO_2/O_2^- with Fe(II)/Fe(III) ions. The reactivity of HO_2/O_2^- with ferric ions and its implication on the occurrence of the Haber-Weiss reaction. *Journal of Physical Chemistry*, **89,** 5062–5066.
38. K. Kobayashi, Y. Harada and K. Hayashi (1991) Kinetic behaviour of the monodehydroascorbate radical studied by pulse radiolysis. *Biochemistry*, **30,** 8310–8315.
39. J.L. Redpath and R.L. Willson (1973) Reducing compounds in radioprotection and radiosensitization: Model experiments using ascorbic acid. *International Journal of Radiation Biology and Related Studies in Physics, Chemistry and Medicine*, **23,** 51–65.
40. B.H.J. Bielski (1978) Reevaluation of the spectral and kinetic properties of $HO_2^{\cdot}$ and $O_2^{\cdot-}$ free radicals. *Photochemistry and Photobiology*, **28,** 645–649.
41. D. Behar, G. Czapski, J. Rabani, L.M. Dorfman and H.A. Schwarz (1970) The acid dissociation constant and decay kinetics of the perhydroxyl radical. *Journal of Physical Chemistry*, **74,** 3209–3213.
42. M.M.T. Khan and A.E Martell (1968) Kinetics of metal ion and metal chelate catalyzed oxidation of ascorbic acid. III. Vanadyl ion catalyzed oxidation. *Journal of the American Chemical Society*, **90,** 6011–6017.
43. M. Nishikimi (1975) Oxidation of ascorbic acid with superoxide anion generated by the xanthine-xanthine oxidase system. *Biochemical and Biophysical Research Communications*, **63,** 463–468.
44. B.H.J. Bielski and H.W. Richter (1977) A study of the superoxide radical chemistry by stopped-flow radiolysis and radiation induced oxygen consumption. *Journal of the American Chemical Society*, **99,** 3019–3023.
45. A.D. Nadezhdin and H.B. Dunford (1979) The oxidation of ascorbic acid and hydroquinone by perhydroxyl radicals. A flash photolysis study. *Canadian Journal of Chemistry*, **57,** 3017–3022.
46. N. Gotoh and E. Niki (1992) Rates of interactions of superoxide with vitamin E, vitamin C and related compounds as measured by chemiluminescence. *Biochimica et Biophysica Acta*, **1115,** 201–207.
47. O.S. Fedorova and V.M. Berdnikov (1978) Radiation-chemical oxidation of ascorbic acid in aqueous solution in the presence of oxygen. *High Energy Chemistry*, **12,** 387–389.
48. D.E. Cabelli and B.H.J. Bielski (1983) Kinetics and mechanisms for the oxidation of ascorbic acid/ascorbate by HO_2/O_2^- radicals. A pulse radiolysis and stopped-flow photolysis study. *Journal of Physical Chemistry*, **87,** 1809–1812.
49. B.H.J. Bielski, A.O. Allen and H.A. Schwarz (1981) Mechanism of disproportionation of ascorbate radicals. *Journal of the American Chemical Society*, **103,** 3516–3518.
50. M. Scarpa, A. Rigo, M. Maiorino, F. Ursini and C. Gregolin (1984) Formation of α-tocopherol radical and recycling of α-tocopherol by ascorbate during peroxidation of phosphatidylcholine liposomes. *Biochimica et Biophysica Acta*, **801,** 215–219.
51. B.H.J. Bielski, R.L. Arudi and M.W. Sutherland (1983) A study of the reactivity of HO_2/O_2 with unsaturated fatty acids. *Journal of Biological Chemistry*, **258,** 4759–4761.
52. E. Cadenas, G. Mernyi and J. Lind (1989) Pulse radiolysis study on the reactivity of trolox C phenoxyl radical with superoxide anion. *FEBS Letters*, **253,** 235–238.
53. R.L. Arudi, M.W. Sutherland and B.H.J. Bielski (1983) Reaction of HO_2/O_2^- with α-tocopherol in ethanolic solutions. In *Oxy radicals and their scavenger systems, Vol. 1, Molecular Aspects* (eds. G. Cohen and R.A. Greenwald), Elsevier, Amsterdam, pp. 26–31. (Referred in[54])
54. B.H.J. Bielski and D.E. Cabelli (1991) Highlights of current research involving superoxide and perhydroxyl radicals in aqueous solutions. *International Journal of Radiation Biology*, **59,** 291–319.
55. Y.A. Vladimirov, V.I. Olenev, T.B. Suslova and Z.P. Cheremisina (1980) Lipid peroxidation in mitochondrial membrane. *Advances in Lipid Research*, **17,** 173–249.
56. R.D. Small Jr., J.C. Scaiano and L.K. Patterson (1979) Radical processes in lipids. A laser photolysis study of t-butoxy radical reactivity toward fatty acids. *Photochemistry and Photobiology*, **29,** 49–51.
57. D.J.W. Barber and J.K. Thomas (1978) Reactions of radicals with lecithin bilayers. *Radiation Research*, **74,** 51–65.
58. C. Evans, J.C. Scaiano and K.U. Ingold (1992) Absolute kinetics of hydrogen abstraction from α-tocopherol by several reactive species including an alkyl radical. *Journal of the American Chemical Society*, **114,** 4589–4593.
59. B. Chance; H. Sies and A. Boveris (1979) Hydroperoxide metabolism in mammalian organs. *Physiological Reviews*, **59,** 527–605.

60. H.J. Forman and I. Fridovich, (1973) Superoxide dismutase: a comparison of rate constants. *Archives in Biochemistry and Biophysics*, **158,** 396–400.
61. E.M. Fielden, P.B. Roberts, R.C. Bray, D.J. Lowe, G.N. Mautner, G. Rotilio and L. Calabrese (1974) The mechanism of action of superoxide dismutase from pulse radiolysis and electron paramagnetic resonance: evidence that only half the actives sites function in catalysis. *Biochemical Journal*, **139,** 49–60.
62. P.B. Roberts, E.M. Fielden, G. Rotilio, L. Calabrese, J.V. Bannister and W.H. Bannister (1974) Superoxide dismutase inactivation by radiation-induced radicals: Evidence for histidine residues in the active site. *Radiation Research*, **60,** 441–452.
63. L. Gebicka and D. Metodiewa (1988) Radiation-induced inactivation of bovine liver catalase in nitrous oxide-saturated solutions. *Journal of Radioanalitical and Nuclear Chemistry*, **127,** 253–260.
64. P. Maruthamuthu and P. Neta (1978) Phosphate radicals. Spectra, acid-base equilibria, and reactions with inorganic compounds. *Journal of Physical Chemistry*, **82,** 710–713.
65. W.A. Pryor, M.J. Kaufman and D.F. Church (1985) Autoxidation of micelle-solubilized linoleic acid. Relative inhibitory efficiences of ascorbate and ascorbyl palmitate. *Journal of Organic Chemistry*, **50,** 281–283.
66. A. Salvador, F. Antunes and R.E. Pinto (1994) 'PARSYS – A package for set-up, simulation and analysis of kinetic models'. Proceedings of the Symposium on Integrative Biochemistry, Abs. 72, Barcelona.
67. S. Wolfram (1988) *Mathematica – A system for doing mathematics by computer.* Addison-Wesley, Reading.
68. L. Petzold (1983) Automatic selection of methods for solving stiff and nonstiff systems of ordinary differential equations. *SIAM Journal on Scientific and Statistical Computing*, **4,** 136–148.
69. K. Hayashi and N. Sakamoto (1986) *Dynamic analysis of enzyme systems – An introduction.* Japan Scientific Societies Press, Tokyo.
70. L.R.C. Barclay, K.A. Baskin, D. Kong and S.J. Locke (1987) Autoxidation of model membranes. The kinetics and mechanism of autoxidation of mixed phospholipid bilayers. *Canadian Journal of Chemistry*, **65,** 2541–2550.
71. Y. Yamamoto, E. Niki, Y. Kamiya and H. Shimasaki (1984) Oxidation of lipids. 7. Oxidation of phosphatidylcholine in homogeneous solution and in water dispersion. *Biochimica et Biophysica Acta*, **795,** 332–340.
72. L.R.C. Barclay, S.J. Locke, J.M. MacNeil, J. vanKessel, G.W. Burton and K.U. Ingold (1984) Autoxidation of micelles and model membranes. Quantitative kinetic measurements can be made by using either water-soluble or lipid-soluble initiators with water-soluble or lipidsoluble chain breaking antioxidants. *Journal of the American Chemical Society*, **106,** 2479–2481.
73. L.R.C. Barclay, S.J. Locke and J.M. MacNeil (1985) Autoxidation in micelles. Synergism of vitamin C with lipid-soluble vitamin E and water-soluble Trolox. *Canadian Journal of Chemistry*, **63,** 366–374.
74. D.C. Liebler, D.S. Kling and D.J. Reed (1986) Antioxidant protection of phospholipid bilayers by α-tocopherol. Control of α-tocopherol status and lipid peroxidation by ascorbic acid and glutathione. *Journal of Biological Chemistry*, **261,** 12114–12119.
75. M. Scarpa, R. Stevanato, P. Viglino and A. Rigo (1983) Superoxide ion as active intermediate in the autoxidation of ascorbate by molecular oxygen. *Journal of Biological Chemistry*, **258,** 6695–6697.
76. T. Doba, G.W. Burton and K.U. Ingold (1985) Antioxidant and co-antioxidant activity of vitamin C, either alone or in the presence of vitamin E or a water-soluble vitamin E analogue, upon the peroxidation of aqueous multilamellar phospholipid liposomes. *Biochimica et Biophysica Acta*, **835,** 298–303.
77. E. Niki, A. Kawakami, Y. Yamamoto and Y. Kamiya (1985) Oxidation of lipids. VIII. Synergistic inhibition of oxidation of phosphatidylcholine liposome in aqueous dispersion by vitamin E and by vitamin C. *Bulletin of the Chemical Society of Japan*, **58,** 1971–1975.
78. M.K. Sharma. and G.R. Buettner (1993) Interaction of vitamin C and vitamin E during free radical stress in plasma: an ESR study. *Free Radical Biology Medicine*, **14,** 649–653.
79. D.D.M. Wayner, G.W. Burton and K.U. Ingold (1986) The antioxidant efficiency of vitamin c is concentration dependent. *Biochimica et Biophysica Acta*, **884,** 119–123.
80. L.R.C. Barclay, S.J. Locke, J.M. MacNeil and J. VanKessel (1985) Quantitative studies of the autoxidation of linoleate monomers sequestered in phosphatidylcholine bilayers. Absolute rate constants in bilayers. *Canadian Journal of Chemistry*, **63,** 2633–2638.
81. Y. Yamamoto, E. Niki, J. Eguchi, Y. Kamiya and H. Shimasaki (1985) Oxidation of biological membranes and its inhibition. Free radical chain oxidation of erythrocyte ghost membranes by oxygen. *Biochimica et Biophysica Acta*, **819,** 29–36.

Accepted by Professor H. Esterbauer